Molecular Cancer Therapeutics

The Preclinical Profile of the Duocarmycin-Based HER2-Targeting ADC SYD985 Predicts for Clinical Benefit in Low HER2-Expressing Breast Cancers

Miranda M.C. van der Lee[1], Patrick G. Groothuis[1], Ruud Ubink[1], Monique A.J. van der Vleuten[1], Tanja A. van Achterberg[1], Eline M. Loosveld[1], Désirée Damming[1], Daniëlle C.H. Jacobs[1], Myrthe Rouwette[1], David F. Egging[1], Diels van den Dobbelsteen[1], Patrick H. Beusker[2], Peter Goedings[3], Gijs F.M. Verheijden[4], Jacques M. Lemmens[4], Marco Timmers[4], and Wim H.A. Dokter[1]

Abstract

SYD985 is a HER2-targeting antibody–drug conjugate (ADC) based on trastuzumab and vc-*seco*-DUBA, a cleavable linker-duocarmycin payload. To evaluate the therapeutic potential of this new ADC, mechanistic *in vitro* studies and *in vivo* patient-derived xenograft (PDX) studies were conducted to compare SYD985 head-to-head with T-DM1 (Kadcyla), another trastuzumab-based ADC. SYD985 and T-DM1 had similar binding affinities to HER2 and showed similar internalization. *In vitro* cytotoxicity assays showed similar potencies and efficacies in HER2 3+ cell lines, but in cell lines with low HER2 expression, SYD985 was 3- to 50-fold more potent than T-DM1. In contrast with T-DM1, SYD985 efficiently induced bystander killing *in vitro* in HER2-negative (HER2 0) cells mixed with HER2 3+, 2+, or 1+ cell lines. At pH conditions relevant for tumors, cathepsin-B cleavage studies showed efficient release of the active toxin by SYD985 but not by T-DM1. These *in vitro* data suggest that SYD985 might be a more potent ADC in HER2-expressing tumors *in vivo*, especially in low HER2-expressing and/or in heterogeneous tumors. In line with this, *in vivo* antitumor studies in breast cancer PDX models showed that SYD985 is very active in HER2 3+, 2+, and 1+ models, whereas T-DM1 only showed significant antitumor activity in HER2 3+ breast cancer PDX models. These properties of SYD985 may enable expansion of the target population to patients who have low HER2-expressing breast cancer, a patient population with still unmet high medical need. *Mol Cancer Ther; 14(3); 692–703. ©2015 AACR.*

Introduction

After many years of investigation, antibody–drug conjugates (ADC) finally find their way to clinical practice (1). The approval of the CD30-targeting ADC brentuximab–vedotin (marketed as Adcetris) for treatment of relapsed Hodgkin lymphoma and relapsed systemic anaplastic large cell lymphoma (2–4) and the more recent approval of ado-trastuzumab emtansine (T-DM1, marketed as Kadcyla) for the treatment of HER2-positive metastatic breast cancer (5–8), confirm the potential of ADCs in cancer treatment. The promise of ADCs as a new class of drugs in oncology is further illustrated by the fact that currently over 30 ADCs are in clinical development and many more are in preclinical programs (1).

The approval of T-DM1 was based on studies demonstrating increased progression-free survival and overall survival time of patients with metastatic HER2-positive breast cancer (5–8) at a dosing regimen (3.6 mg/kg/3 weeks) that was well tolerated. The introduction of T-DM1 has added great value to the therapeutic armamentarium for patients with HER2-positive metastatic breast cancer; nevertheless, the patient population that might benefit from a HER2-targeting ADC could be expanded by a more effective HER2-targeting ADC. T-DM1 is approved for the treatment of HER2-positive metastatic breast cancers, defined as IHC-HER2 3+ or FISH-positive/IHC-HER2 2+. According to these criteria, approximately 20% to 25% of all metastatic breast cancer patients are currently eligible for T-DM1 therapy (9, 10). A HER2-targeting drug that has a clinical benefit in patients whose tumor is FISH-negative but has detectable IHC HER2 expression (2+ and 1+) would at least double that population (10, 11).

We recently described SYD985, a new HER2-targeting ADC based on the cleavable linker-duocarmycin payload, valine-citrulline-*seco* DUocarmycin hydroxyBenzamide Azaindole (vc-*seco*-DUBA), conjugated to trastuzumab (12). SYD985, and its unfractionated precursor SYD983, showed high antitumor activity in HER2-positive breast cancer patient-derived xenograft (PDX) models in mice (12). To further assess the potential of SYD985, a series of mechanistic *in vitro* studies and breast

[1]Department of Preclinical, Synthon Biopharmaceuticals, Nijmegen, the Netherlands. [2]Department of Medicinal and Protein Chemistry, Synthon Biopharmaceuticals, Nijmegen, the Netherlands. [3]Department of Medical R&D, Synthon Biopharmaceuticals, Nijmegen, the Netherlands. [4]Department of New Molecular Entities, Synthon Biopharmaceuticals, Nijmegen, the Netherlands.

Note: Supplementary data for this article are available at Molecular Cancer Therapeutics Online (http://mct.aacrjournals.org/).

Corresponding Author: Wim H.A. Dokter, Synthon Biopharmaceuticals, Microweg 22, 6503 GN Nijmegen, the Netherlands. Phone: 31-24-372-7700; Fax: 31-24-372-7705; E-mail: Wim.Dokter@Synthon.Com

doi: 10.1158/1535-7163.MCT-14-0881-T

cancer PDX studies were initiated to directly compare the antitumor activity of SYD985 with T-DM1 in models with different HER2 status. The preclinical profile described in the present paper supports clinical studies with SYD985, particularly studies that aim at extending the target population to patients with metastatic breast cancer tissue that has FISH-negative/IHC-HER2 2+ and 1+ status.

Materials and Methods

SYD985 and T-DM1

SYD985 was prepared as described previously (12–15). Two batches of T-DM1 from Roche were obtained, EU batch N0001B02 and US batch 535405. Both batches of T-DM1 showed similar *in vitro* potency and efficacy data on a panel of four human tumor cell lines (Supplementary Fig. S1). Head-to-head studies comparing T-DM1 with SYD985 in this paper were conducted with batch N0001B02.

Cancer cell lines and quantification of HER2 levels

Within the period 2011–2014, human tumor cell lines SK-BR-3, UACC-893, NCI-N87, SK-OV-3, MDA-MB-175-VII, ZR-75-1, NCI-H520, and SW-620 were obtained from ATCC. No further cell-line authentication was conducted. NCI-N87, ZR-75-1, MDA-MB-175-VII, SW-620, and NCI-H520 cells were cultured in RPMI-1640 media (Lonza) supplemented with 10% v/w FBS, which was heat inactivated (HI; Gibco- Life Technologies), at 37°C in a humidified incubator containing 5% CO_2. SK-BR-3 and SK-OV-3 cells were maintained in McCoys 5A medium (Lonza) containing 10% v/w FBS HI, and UACC-893 cells were cultured in DMEM/F-12, Glutamax supplement (Gibco-Life Technologies) containing 20% v/w FBS (Gibco-Life Technologies).

HER2/neu antigen expression on the surface of human tumor cell lines was quantified using the DAKO Qifikit (DAKO), according to the manufacturer's protocol.

Cell viability assays

Cells in complete growth medium were plated in 96-well plates (90 μL/well) and incubated at 37°C, 5% CO_2 at the following cell densities: 6500 SK-BR-3, 10000 UACC-893, 10000 NCI-N87, 2000 SK-OV-3, 2500 MDA-MB-175-VII, 2500 ZR-75-1, 4000 SW-620, and 5000 NCI-H520 cells per well. After an overnight incubation, 10 μL of mAb, drug, and/or active toxin (*seco*-DUBA) was added. Serial dilutions were made in culture medium. For the studies with a shorter exposure of the ADCs, cells were washed once with complete growth medium after 6 and 24 hours, followed by addition of 100 μL of the same medium. Cell viability was assessed after 6 days, unless indicated otherwise, using the CellTiter-Glo (CTG) luminescent assay kit from Promega Corporation according to the manufacturer's instructions and as detailed previously (12). Percentage survival was calculated by dividing the measured luminescence for each drug or ADC concentration with the average mean of untreated cells (only growth medium) multiplied by 100.

Fluorescent labeling of SYD985 and T-DM1

SYD985 and T-DM1 were labeled with an Alexa Fluor 488 reactive dye from Invitrogen, which has a tetrafluorophenyl ester moiety that reacts efficiently with primary amines of proteins to form stable dye–protein conjugates. Before labeling, T-DM1 or SYD985 was desalted into PBS and the protein concentration was determined using UV absorbance at 280 nm. The pH was adjusted to pH 8.3 and labeling was performed by incubation of T-DM1 or SYD985 solution with an Alexa Fluor 488 solution in DMA in a 9:1 molar ratio (dye:mAb) for 1 hour. After incubation, labeled T-DM1 or SYD985 was buffer exchanged into PBS using gel filtration. The degree of labeling was calculated from the UV absorbance at 280 and 495 nm according to the documentation supplied with the labeling kit and was found to be 1.4 for SYD985 and 1.8 for T-DM1.

Internalization studies

Internalization was performed as detailed previously (11). Cells (2,000,000 cells/tube) were incubated for 1 hour at 4°C with 2 mL of 3 μg/mL Alexa Fluor 488 (AF488)-labeled SYD985 or 2 mL of 3 μg/mL Alexa Fluor 488-labeled T-DM1. These cells were split into two groups after a wash step with ice-cold 1× PBS (Lonza) containing 0.2% v/w BSA (Sigma-Aldrich). For one part of the cells, internalization was assessed upon incubation at 37°C (100 μL cell solution/vial). The other part was used as control cells for the total cell surface binding and was incubated at 4°C. After the indicated incubation times, cells were washed three times with ice-cold 1× PBS-0.2% v/w BSA buffer. The remaining surface expression was visualized after quenching with 50 μL of anti-Alexa Fluor 488 Rabbit IgG Ab (1:30 dilution; Molecular Probes, Life Technologies) for 30 minutes at 4°C. Fluorescence intensities were determined by flow cytometry (BD FACSVerse) and indicated as the median fluorescence intensity (MFI). Internalization was quantified by calculating the percentage of internalization with the following formula: MFI of the internalized signal (surface AF488-labeled ADC quenched by anti-AF488 and corrected for untreated cells) divided by the total bound AF488-labeled ADC (unquenched cells corrected for untreated cells) multiplied with 100.

Enzymatic cleavage by cathepsin B

0.1 mg/mL of the ADC or 10 μmol/L active toxin (*seco*-DUBA) was mixed with 5 μg/mL human liver cathepsin B (Calbiochem) in 0.1 mol/L Na-acetate buffer, pH 5, 6, 6.5 or 7, supplemented with 4 mmol/L DTT. As a control, ADCs or *seco*-DUBA was diluted in culture medium to a 0.1 mg/mL concentration. After 4 hours of preincubation at 37°C, serial dilutions were made from each stock solution in culture medium and 10 μL was added to each well of a 96-wells plate. SW-620 cells (90 μL; 4,000 cells/well) were cultured with these ADCs or *seco*-DUBA for 6 days, and the cell viability was measured after 6 days using the CTG assay kit.

Bystander killing assay

HER2-positive SK-BR-3, SK-OV-3, or MDA-MB-175-VII cells were mixed with HER2-negative NCI-H520 cells in McCoy's 5A medium containing 10% v/w FBS HI. Five thousand cells per well of each cell type (1:1 ratio), or indicated otherwise, were added to a 96-well plates (90 μL/well). Single cultures were seeded at a density of 5,000 cells/well (90 μL/well). After 4 hours, 10 μL of each ADC or *seco*-DUBA was added. Serial dilutions were made in culture medium. Cell viability was assessed after 6 days, unless indicated otherwise, using the CTG luminescent assay kit.

Bystander FACS analyses

NCI-H520 cells were labeled with CellTrace Violet (Life Technologies) according to the manufacturer's instructions. Similar as to the bystander killing studies, a 1:1 ratio of HER2-positive and

HER2-negative cells were mixed (10,000 cells/well of each cell type) and plated in 96-well plates (90 μL/well). Single cultures were seeded at a density of 10,000 cells/well (90 μL/well). After an overnight incubation, 10 μL of 1 μg/mL ADC or (*seco*-pro) drug was added. Cells were detached with 0.1%-trypsin-EDTA after the indicated incubation time and washed with FACS buffer (ice-cold 1× PBS containing 0.2% v/w BSA). Pellet was resuspended in 150 μL FACS buffer supplemented with 0.7 μmol/L TO-PRO-3 Iodide (Life Technologies). Fluorescence intensities were determined for 1 minute using the high-sensitivity mode on the BD FACSVerse. The CellTrace violet labeled NCI-H520 cells allowed detection and gating between the HER2-negative labeled NCH-H520 cells and the HER2-positive nonlabeled cells. Dead cells were gated using TO-PRO-3 Iodide. The percentage of gated viable cells was calculated on the basis of the total cell population (viable plus dead cells is 100%).

Cleavage by CES1c

A 100 μg/mL concentration of SYD985 was spiked in human K2-EDTA plasma together with 0, 10, 100, 200, and 400 μg/mL recombinant mouse carboxylesterase 1c (CES1c, Cusabio Biotech). After 96 hours of incubation at 37°C, plasma samples were snap frozen in liquid nitrogen and stored at −80°C until bioanalysis. SYD985 ADC (conjugated antibody) levels and total antibody (TAb) levels in plasma were quantified using an ELISA-based method as described previously (12).

Cell line and patient-derived xenograft studies

The *in vivo* antitumor activity of SYD985 versus T-DM1 was tested as single-dose therapy in the BT-474 cell line-derived xenograft model, and a selection of breast cancer PDX. The BT-474 model was performed at Oncodesign. PDX models used were MAXF 1162, MAXF MX1, and MAXF 449 (Oncotest), ST313 (South Texas Accelerated Research Therapeutics), HBCx-34 and HBCx-10 (Xentech). Initial tumor volumes at the day of randomization and treatment ranged from 52 to 379 mm^3. All studies were approved by the local animal care and use committees according to established guidelines. The HER2 FISH and IHC status of the BT-474 tumor and tumors from the PDX models as determined by the CROs were independently confirmed as described below in this Materials and Methods section. The characteristics of all tumors used in this paper are summarized in Supplementary Table S1. Representative photographs of the HER2 IHC staining are presented in Supplementary Fig. S2. Studies were conducted as detailed previously (12).

HER2 gene amplification

HER2/neu gene amplification was determined by *in situ* hybridization (ISH) in formalin-fixed, paraffin-embedded human breast cancer tissue specimens with a Ventana-Roche automated platform and an inform HER2 Dual ISH DNA probe cocktail, UltraView SISH DNP Detection kit, and UltraView Red ISH Dig detection kit, as detailed by the supplier.

HER2 IHC staining

Tissue sections of formalin-fixed paraffin-embedded tumor xenograft samples were prepared. IHC was performed on the Discovery automated platform (Ventana-Roche) with the primary Ab anti-HER2/neu (4B5) rabbit monoclonal (Ventana-Roche, ref 790-4493) and the detection kit OmniMap RB HRP (anti-rabbit multimer, Ventana-Roche reference 760-4311) associated to the chromogenic kit ChromoMap DAB (Ventana-Roche reference 760-159, as detailed by the supplier.

PK studies and bioanalytical assays

BT-474 tumor-bearing female balb/c nu/nu mice and female cynomolgus monkeys were dosed intravenously with 1, 3, and/or 5 mg/kg SYD985 or T-DM1. Blood samples were taken at multiple time point hours after dosing, cooled on ice water, and processed to plasma as soon as possible. Plasma samples were snap frozen in liquid nitrogen and stored at −80°C until bioanalysis. SYD985 ADC (conjugated antibody) levels and TAb levels in plasma were quantified using an ELISA-based method as described previously (12). The conjugated antibody assay uses an anti-toxin antibody as solid phase and a biotinylated anti-idiotype mini antibody for detection. In the TAb assay, the anti-idiotype mini-antibody is used as solid phase instead of the anti-toxin antibody. A validated LC/MS-MS based method was used for quantification of active toxin (DUBA) in plasma. A competitive EIA-based method (KTR 756 DM1 ADC EIA kit, Epitope Diagnostics) was used for the determination of T-DM1 levels in plasma according to the protocol of the supplier.

Statistical analysis

Statistical analyses of *in vitro* cytotoxicity assays and *in vivo* xenograft experiments were performed as detailed previously (12).

Results

SYD985

SYD985 (Fig. 1) was synthesized and prepared as described previously (12). In short, vc-*seco*-DUBA was coupled to cysteine residues of trastuzumab after partial reduction of the interchain disulfides. SYD985 was further purified by hydrophobic interaction chromatography to deliver a well-defined ADC consisting of predominantly species with a drug to antibody ratio (DAR) of 2 and 4, yielding a mean DAR of 2.8. Some crucial features of the antibody, such as binding affinity and induction of ADCC activity *in vitro* were not affected by conjugation (data not shown) as was also published for SYD983, the unfractionated form of SYD985 (12).

Binding and internalization of SYD985 and T-DM1

Binding capacity and percentage of internalization of SYD985 and T-DM1 were determined in time using flow-cytometric analyses in cell lines SK-BR-3 (breast carcinoma), SK-OV-3 (ovarian carcinoma), and MDA-MB-175-VII (breast carcinoma), which are classified as HER2 3+, 2+, and 1+, respectively. SYD985 and T-DM1 showed a similar binding activity (EC_{50} 0.4–0.9 μg/mL) to cell surface HER2, irrespective of the HER2 expression level. The rank order of maximum binding capacity of both SYD985 and T-DM1 correlated with the number of HER2-binding sites on the tumor cells. Receptor-mediated endocytosis of Alexa Fluor 488 (AF488)-labeled SYD985 into HER2-positive tumor cells was compared with the uptake of AF488-labeled T-DM1. Fluorescence of each internalized ADC was measured by flow cytometry after quenching of the surface-bound AF488-labeled ADC with an anti-AF488 antibody. A limitation of this approach is the incomplete quenching of the cell-surface bound AF488-labeled ADCs, as is evident from the 4°C controls. This is in line with the supplier instructions that described a maximum

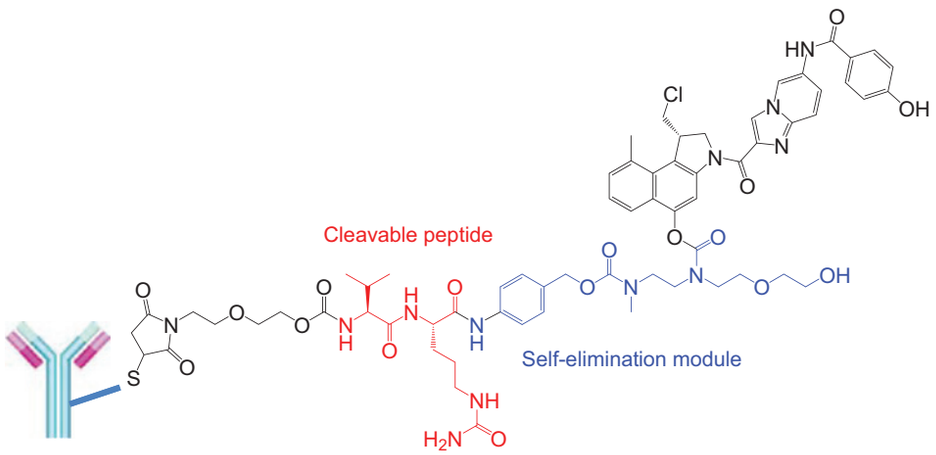

Figure 1.
Structure of SYD985.

quenching of the AF488 dye up to 90% or lower in the case of conjugated AF488 dye. The kinetics of uptake for SYD985 and T-DM1 were comparable. Also the maximum percentages of internalization for both ADCs are within the same order of magnitude (Fig. 2A).

Cytotoxicity of SYD985 versus T-DM1 *in vitro*

A set of eight cell lines was selected on the basis of their published HER2 status; breast carcinomas SK-BR-3 and trastuzumab-resistant UACC-893 (both HER2 3+), gastric carcinoma NCI-N87 (HER2 3+), ovarian carcinoma SK-OV-3 (HER2 2+), breast carcinomas MDA-MB-175-VII and ZR-75-1 (both HER2 1+), and metastatic colon carcinoma SW-620 and lung adenocarcinoma NCI-H520 (both HER2 0). The HER2 status of these cell lines was confirmed by Qifi-kit analysis (Supplementary Fig. S3). We have previously (12) shown that SK-BR-3, SK-OV-3, SW-620, and NCI-H520 all are highly sensitive to the active toxin *seco*-DUBA, decreasing the cell viability with potencies between 0.08 nmol/L and 0.4 nmol/L after a 6-day treatment. Cytotoxicity studies in NCI-N87 and UACC-893 cell lines, confirmed high sensitivity to *seco*-DUBA with potencies of 0.2 nmol/L (Supplementary Fig. S4A). Because *seco*-DUBA was less potent against MDA-MB-175-VII (2.5 nmol/L) and ZR-75-1 (8.2 nmol/L) cells at 6 days, we extended the treatment time up to 12 days with corresponding IC_{50} values of 0.1 and 0.2 nmol/L, respectively (Supplementary Fig. S4A). As shown in Fig. 2B, SYD985 and T-DM1 demonstrate similar potencies in the HER2 3+ cell lines SK-BR-3, UACC-893, and NCI-N87. IC_{50} values are 6.9 and 15.7 ng/mL in SK-BR-3, 54.1 and 35.9 ng/mL in UACC-893, and 24.5 and 44.9 ng/mL in NCI-N87, for SYD985 and T-DM1, respectively. Although SYD985 and T-DM1 both potently kill UACC-893 cells, we confirmed lack of responsiveness to trastuzumab (Supplementary Fig. S4B; refs. 16, 17). Importantly, SYD985 retained its activity in cell lines with lower HER2 expression, whereas T-DM1 became less potent with IC_{50} values of 32.4 and 112.1 ng/mL in SK-OV-3, 67.4 and 313.9 ng/mL in MDA-MB-175-VII, and 14.9 and >1,000 ng/mL in ZR-75-1, for SYD985 and T-DM1, respectively (see Supplementary Table S2 for the percentage efficacy and 95% confidence intervals). Neither SYD985 nor T-DM1 was able to kill HER2-negative SW-620 or NCI-H520 cells (Fig. 2B), indicating that both ADCs mediate their cytotoxic effect through HER2. Thus, overall these data show that in cell lines with lower HER2 expression (HER2 2+/1+), SYD985 is significantly (factor 3–50) more potent than T-DM1.

Next, we studied the relation between exposure times to ADC and cell killing after 6 days, in three cell lines with different HER2 expression levels. SK-BR-3, SK-OV-3, and MDA-MB-175-VII cells were exposed to SYD985 and T-DM1 for 6 and 24 hours, washed to remove ADCs, and cultured until 6 days, except for MDA-MB-175-VII cells (12 days). As control, cells were treated with ADCs during the entire incubation of 6 and 12 days. A short incubation of 6 hours was enough for both SYD985 and T-DM1 to potently kill SK-BR-3 cells after 6 days, indicating that sufficient amounts of the respective toxins were loaded inside cells to induce killing (Fig. 2C). For SK-OV-3 and MDA-MB-175-VII cells, in line with their lower HER2 expression, a 6- or even 24-hour exposure to ADC did not induce maximum killing, suggesting that recycling of HER2 after internalization and reloading of cells with ADC is needed for potent killing of cells with low HER2 levels (Fig. 2C).

Protease sensitivity and bystander killing *in vitro*

Proteases, like cathepsin B, are highly expressed in a wide variety of tumors, including breast cancer tumors, and can also be active extracellularly through secretion by malignant cells (18, 19). The sensitivity of SYD985 and T-DM1 to cathepsin B cleavage was evaluated at pH 5 to mimic the acidic milieu in lysosomes and at pH 6, 6.5, and 7 to mimic pH in endosomes and tumor environment. SYD985 and T-DM1 were exposed for 4 hours to activated cathepsin B and release of active toxin was quantified by measuring cytotoxic activity on HER2-negative SW-620 cells. In the absence of cathepsin B, SYD985 did not reduce cell viability of SW-620 cells. However, 4 hours preincubation of SYD985 with cathepsin B, in a pH range between 5 to 7, resulted in potent killing of SW-620 cells, indicating release of active toxin (Fig. 3A). Preincubation of T-DM1 with cathepsin B did not result in cytotoxic activity (Fig. 3A), which is in line with the nature of its noncleavable thioether linker. These data show that SYD985, most likely through its valine-citrulline motif, and in contrast with T-DM1, rapidly releases active toxin through cathepsin B cleavage, an enzyme abundantly present in the tumor cell and microenvironment. In mice, an enzyme present in plasma can cleave vc-*seco*-DUBA and cause release of active toxin. Adding 1% mouse plasma causes a dramatic shift in cytotoxic activity of SYD985 on

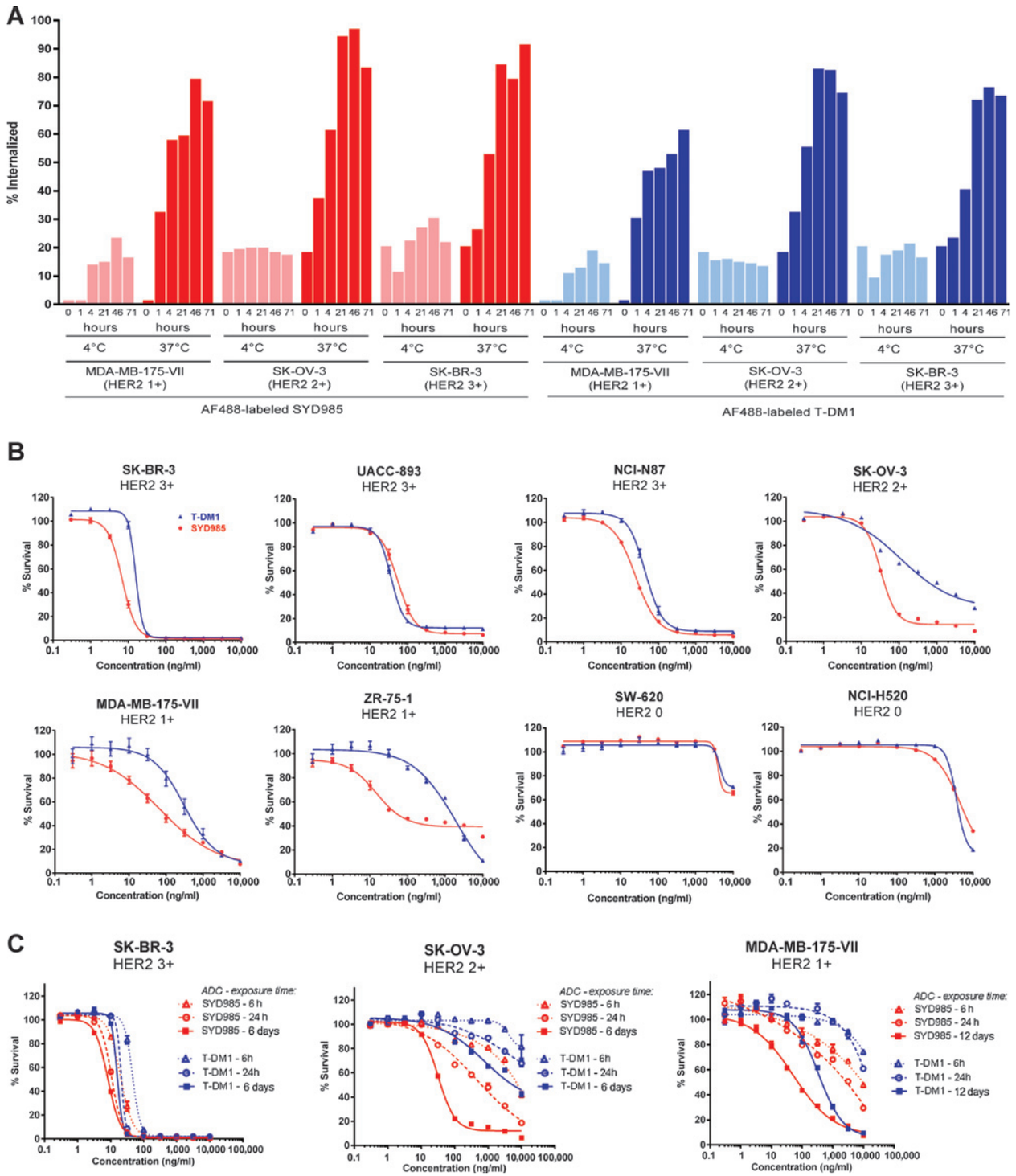

Figure 2.
In vitro profile of SYD985. A, percentage of internalization in time (0, 1, 4, 21, 45, and 71 hours) for SYD985 and T-DM1 on HER2 3+, 2+, and 1+ tumor cells. B, cytotoxicity induced by SYD985 (in red) and T-DM1 (in blue) on a panel of eight human tumor cell lines with different HER2 levels. C, cytotoxicity induced after 6 and 24 hours of exposure to SYD985 (in red) and T-DM1 (in blue) on HER2 3+, 2+, and 1+ cells, followed by a wash step and the remaining incubation time.

HER2-negative SW620 cells, in contrast with human plasma (Fig. 3A). *In vitro* incubation of SYD985 with recombinant mouse carboxylesterase 1C does release this active species as well (Supplementary Fig. S4B), suggesting that in mouse plasma, carboxylesterase 1C might be responsible for cleavage of vc-*seco*-DUBA. The position at which this cleavage occurs is

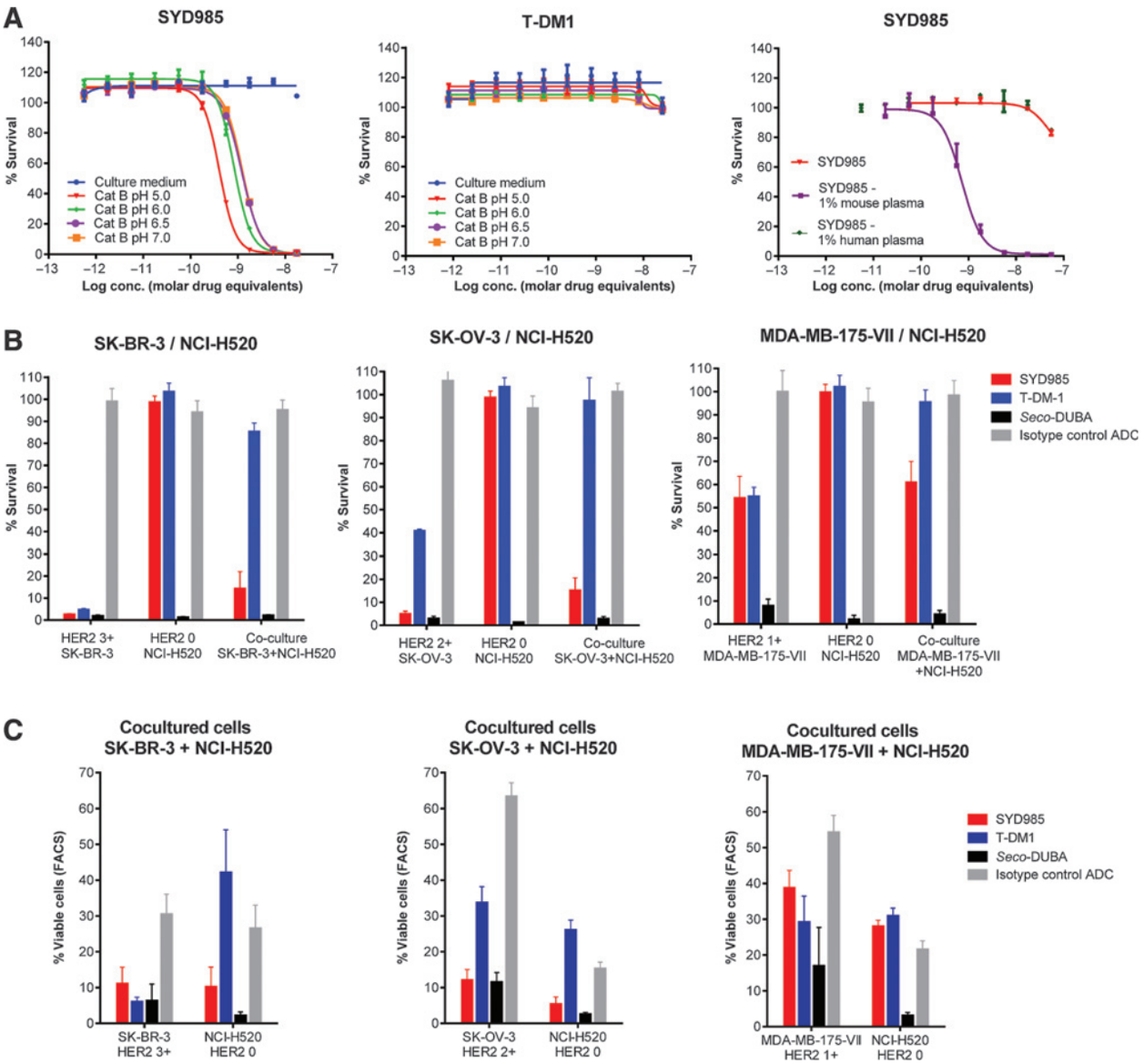

Figure 3.
In vitro cathepsin B sensitivity, stability in mouse plasma, and bystander killing. A, cytotoxic activity of released active toxin on HER2-negative SW-620 cells after 4-hours exposure of SYD985 and T-DM1 to cathepsin B, and when SYD985 is exposed to 1% mouse or human plasma supplemented to the culture medium. B, cytotoxicity induced on HER2-positive, HER2-negative, and cocultured cells after treatment of 6 days with 1 μg/mL of ADCs or 10 nmol/L of active toxin using the CTG luminescence assay. Percentage survival was calculated related to total untreated viable cells. C, percentage of HER2-positive and HER2-negative gated viable cells in the cocultured cell population detected by FACS analysis. Dead cells identified by TO-PRO-3 Iodide were part of the total cell population (is 100%; bars not shown). NCI-H520 cells were labeled with CellTrace Violet allowing detection and gating of each cell type.

most likely the carbamate group connecting the alkylating moiety of the duocarmycin to the linker (Fig. 1) since previous studies with valine-citrulline linkers have indicated that this site is quite stable in mouse plasma (20).

Next, the ability of SYD985 and T-DM1 to kill HER2-negative bystander tumor cells was explored. NCI-H520 (HER2 0) cells were cocultured (5,000 cells of each cell type per well) with one of the following HER2-positive cell lines, SK-BR-3 (HER2 3+), SK-OV-3 (HER2 2+), or MDA-MB-175-VII (HER2 1+). Cells were treated for 6 days with either SYD985, its nonbinding isotype control ADC, T-DM1, or the active toxin *seco*-DUBA. NCI-H520 cells were insensitive (IC_{50} > 50 nmol/L) to SYD985, its isotype control ADC, and T-DM1 but were sensitive for *seco*-DUBA (IC_{50} 0.04 nmol/L; Fig. 3B and Supplementary Fig. S4D). As shown in Fig. 3B, treatment of SK-BR-3/NCI-H520 and SK-OV-3/NCI-H520 cocultures with 1 μg/mL SYD985 resulted in killing of the HER2 0 NCI-H520 cells, whereas the nonbinding isotype control ADC and T-DM1 did not. Coculturing of cells for 6 days resulted in a dissimilar distribution of the percentage of viable HER2-positive and HER2-negative cells, which was indicated by the results of the isotype control ADC and is most likely due to differences in growth rates.

Despite these differences in growth rates, FACS confirmed (Fig. 3C) that in the presence of SYD985, HER2 0 cells were killed when cocultured with SK-BR-3 and SK-OV-3 cells, and not in the presence of T-DM1. Bystander killing in the MDA-MB-175-VII/NCI-H520 coculture was not so evident after 6 days of incubation, but became clearly visible after 12 days of incubation (Supplementary Fig. S5A). To strengthen these bystander killing studies, we determined the minimum proportion of HER2 3+ target cells required for SYD985-mediated bystander killing of HER2 0 cells. Different ratios of HER2-positive SK-BR-3 and HER2-negative NCI-H520 cells were cocultured, resulting in 100%, 80%, 60%, 40%, 20%, and 0% HER2-positive cells (Supplementary Fig. S5B). With only 20% of HER2 3+ target cells, SYD985 was still able to kill 65% of the mixed cell population indicating bystander killing. In contrast, under the same condition, in which 20% of the HER2 3+ target cells are present, T-DM1 was able to kill 9% of the cocultured cells (Supplementary Fig. S5B).

These findings indicate that active toxins are released after processing of SYD985 by HER2-positive cells that are either HER2 3+, 2+, or 1+, resulting in the killing of HER2 0 cells in the immediate vicinity. These results are consistent with previously reported results showing that at least some cleavable linkers could facilitate bystander killing, whereas a noncleavable ADC was not able to kill antigen-negative bystander cells (21, 22).

Taken together, this *in vitro* profile indicates that SYD985 might show more antitumor potential than T-DM1, especially in tumors that express low levels of HER2 and/or are heterogeneous in their HER2 expression.

In vivo antitumor activity of SYD985 versus T-DM1

In vivo antitumor activity of SYD985 versus T-DM1 was tested in a cell line (BT-474) xenograft and a range of breast cancer PDX models, with different HER2 status. After single-dose administration, tumor growth was inhibited in a dose-dependent manner in the BT-474 cell line xenograft model and the MAXF1162 breast cancer PDX model (both HER2 3+; Fig. 4A and B). SYD985 is significantly more active (7 out of 8 mice showed complete tumor remission with SYD985 at 5 mg/kg vs. none for T-DM1) than T-DM1 in these models. In contrast with 1 mg/kg T-DM1, 1 mg/kg SYD985 significantly reduced tumor volume compared with the vehicle group in the BT-474 xenograft, and based on the AUCs (tumor volume vs. time) of the tumor size data, 5 mg/kg SYD985 is significantly more active ($P = 0.0148$) than 5 mg/kg T-DM1. In MAXF 1162, also a HER2 3+ tumor, there was no statistically significant difference between AUCs of the 10 mg/kg groups at the end of the study (day 72). In FISH negative/IHC HER2 2+ breast cancer PDX models, SYD985 was consistently more active than T-DM1 (Fig. 4C and D). The difference was most apparent in the HBCx-34 model (Fig. 4D) showing a complete response in 1 out of 8 mice at 3 mg/kg SYD985 and in 4 out of 8 mice when treated with 10 mg/kg. T-DM1 was not active. In the FISH-negative/IHC 1+ MAXF 449 model (Fig. 4E), SYD985 was dosed in a lower range: 0.3, 1, and 3 mg/kg, and it was observed that 1 and 3 mg/kg SYD985 showed similar efficacy compared with 30 mg/kg T-DM1. Remarkably, in two other FISH-negative/IHC HER2 1+ triple-negative breast cancer PDX models MAXF-MX1 and HBCx-10, SYD985 appeared to be particularly active (Fig. 4F and G). In MAXF-MX1 (Fig. 4F), 4 out of 6 mice in the 1 mg/kg group showed a complete response to SYD985, at 3 mg/kg all, mice had complete tumor remission. In the HBCx-10 (Fig. 4G), 4 out of 7 mice showed a complete response at 1 mg/kg as did all mice in the 3 mg/kg group. In contrast, T-DM1, even when dosed up to 30 mg/kg, showed no significant antitumor activity in these models.

The nonbinding isotype control ADC, which is vc-*seco*-DUBA conjugated to rituximab (prepared with a similar protocol as SYD985 and with similar DAR and HIC profile), showed, at similar dosages, significantly less antitumor activity than SYD985 in the HER2 3+ xenograft models (Fig. 5A and B), indicating that the effect of SYD985 is largely HER2 mediated. Like for the BT-474 and MAXF1162, also for both the HER2 2+ PDX models, antitumor activity of the nonbinding ADC was observed, illustrative of a bystander effect. However, at the lower dosages, HER2-mediated effects clearly contributed to the antitumor activity of SYD985 (Fig. 5C and D). At higher dose (10 mg/kg), this difference between isotype control ADC and SYD985 was no longer apparent in tumor model ST313 (Fig. 5C). Finally, also for the three FISH-negative/IHC 1+ models, SYD985-mediated antitumor effects could be attributed to be largely due to HER2-mediated effects. Effects induced by the isotype control ADC indicated for nontarget mediated antitumor activity as well (Fig. 5E–G).

In all PDX studies, in all experimental groups, body weight was determined twice a week as a measure for toxicity and potential overdosing. None of the animals in any of the experimental groups in any of the PDX studies showed significant change in body weight.

Taken together, these data show that, in contrast with T-DM1, SYD985 is active in breast cancer PDX models with low (2+ and 1+) HER2 status.

Plasma kinetics

In vivo plasma kinetics of SYD985 and T-DM1 were studied in BT-474 tumor-bearing mice, since, in contrast with results reported for T-DM1 (23, 24), we observe a difference in PK between tumor-bearing mice and healthy balb/c mice (12). This is probably caused by target mediated drug disposition, dependent on HER-2 expression levels in the tumor model used, and dependent on the degree of saturation of HER-2 target molecules at the given dose.

As shown in Fig. 6A and Supplementary Table S3, SYD985 shows high clearance of conjugated antibody (18.2–19.7 mL/hour/kg). This is in line with sensitivity of vc-*seco*-DUBA–based ADCs to esterase activity in mouse plasma. This sensitivity for esterases is mouse CES1c specific, because SYD985 shows high *in vitro* stability in plasma from CES1c knockout mice, human, and monkey plasma (12). Furthermore, these findings were confirmed *in vivo*, showing low clearance of conjugated antibody in CES1c knockout mice (0.51 mL/hour/kg; Supplementary Fig. S6) and monkey (0.52 mL/hour/kg). Remarkably, in monkey, conjugated antibody levels were hardly different from TAb concentrations (clearance of 0.38 mL/hour/kg) and T-DM1 concentrations (clearance of 0.64 mL/hour/kg; ref. 25), while active toxin (DUBA) plasma levels remain extremely low (Fig. 6B). Mean Cmax DUBA level was 0.018 ng/mL versus 5.85 ng/mL for DM1 (25), both dosed at 3 mg/kg ADC in female monkeys.

After T-DM1 administration to mice, ADC clearance is much lower (1.8–1.7 mL/hour/kg) compared with SYD985 (Fig. 6A and Supplementary Table S3). This is in line with published

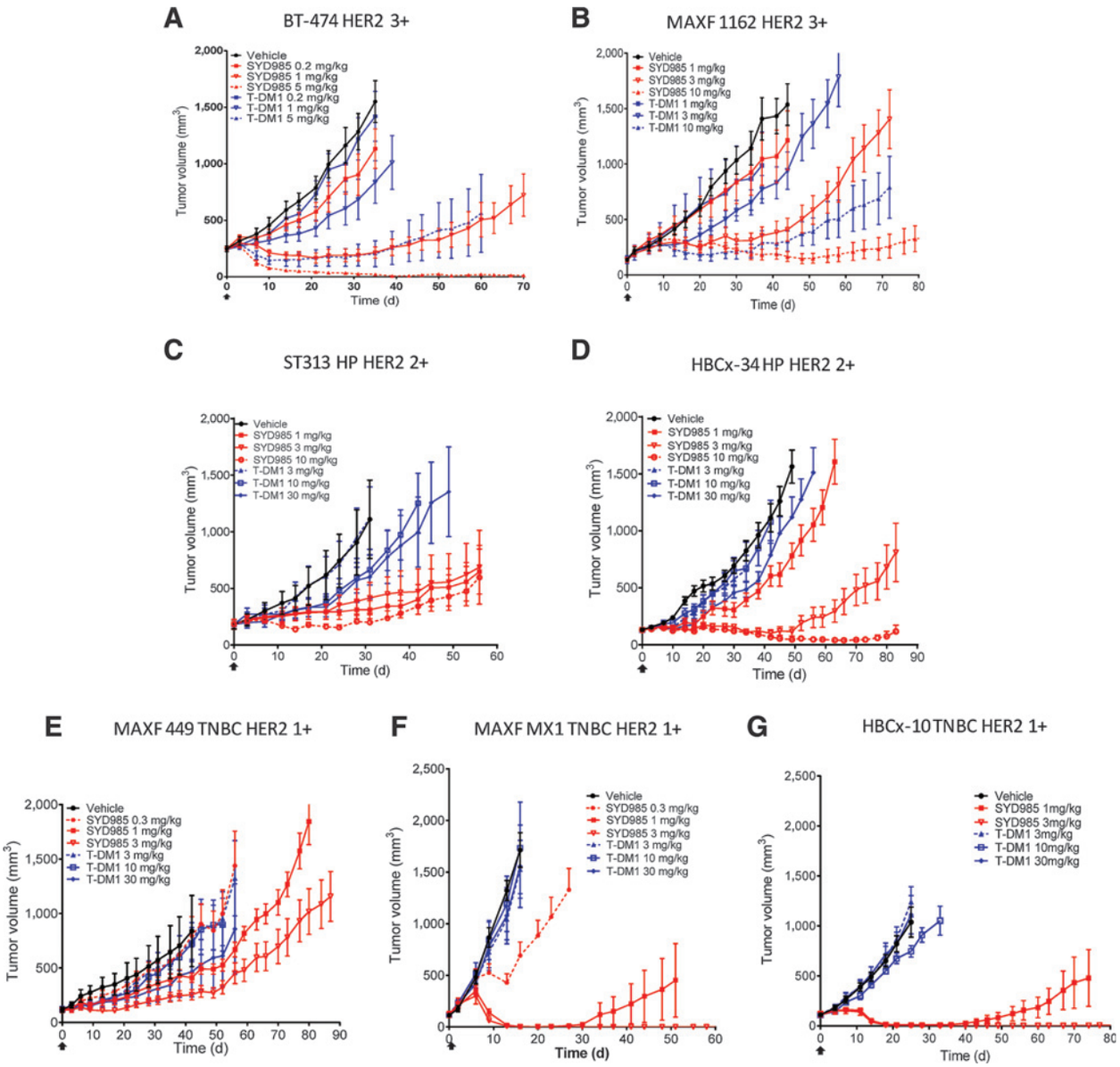

Figure 4.
Antitumor activity of SYD985 compared with T-DM1 in BT-474 xenograft tumor model (A) and in breast cancer PDX with different levels of HER2 expressions (B–G). Mice were treated with a single dose administered intravenously as indicated by the arrow on the *x*-axis (A–G). Data of isotype control ADC are shown in Fig. 5.

PK data for T-DM1 (24) showing a clearance of 0.75 to 0.9 mL/hour/kg for T-DM1, especially when taking into account that the tumor model used shows higher clearance compared with non-tumor-bearing mice. Unfortunately, a true quantitative comparison of ADC exposure after dosing of T-DM1 or SYD985 is not possible due to differences between and limitations of the bioanalytical tools. Nevertheless, it is clear that SYD985 shows much higher ADC clearance, most likely due to esterase mediated cleavage of the linker drug, although it cannot be ruled out that other causes of deconjugation, like maleimide exchange to albumin, may contribute. As a consequence, a higher formation of naked antibody is seen for SYD985 compared with T-DM1 in mice.

Mechanism of antitumor activity *in vivo*

To evaluate whether the early release of *seco*-DUBA in mouse plasma after dosing of SYD985 might affect or contributes to antitumor activity, we performed a predosing study in the MAXF-MX1 and HBCx-34 PDX models. In both models, a pretreatment of 24 hours with a high dose of trastuzumab blocked antitumor activity of an active dose of SYD985 (Fig. 6C and D). These data confirm for these two models the earlier conclusion that HER2-mediated targeting to the tumor is essential for antitumor activity. It furthermore proves that antitumor activity of SYD985 at least in these two models is not driven by the early release of active toxin in mouse plasma as a result of mouse carboxylesterase cleavage.

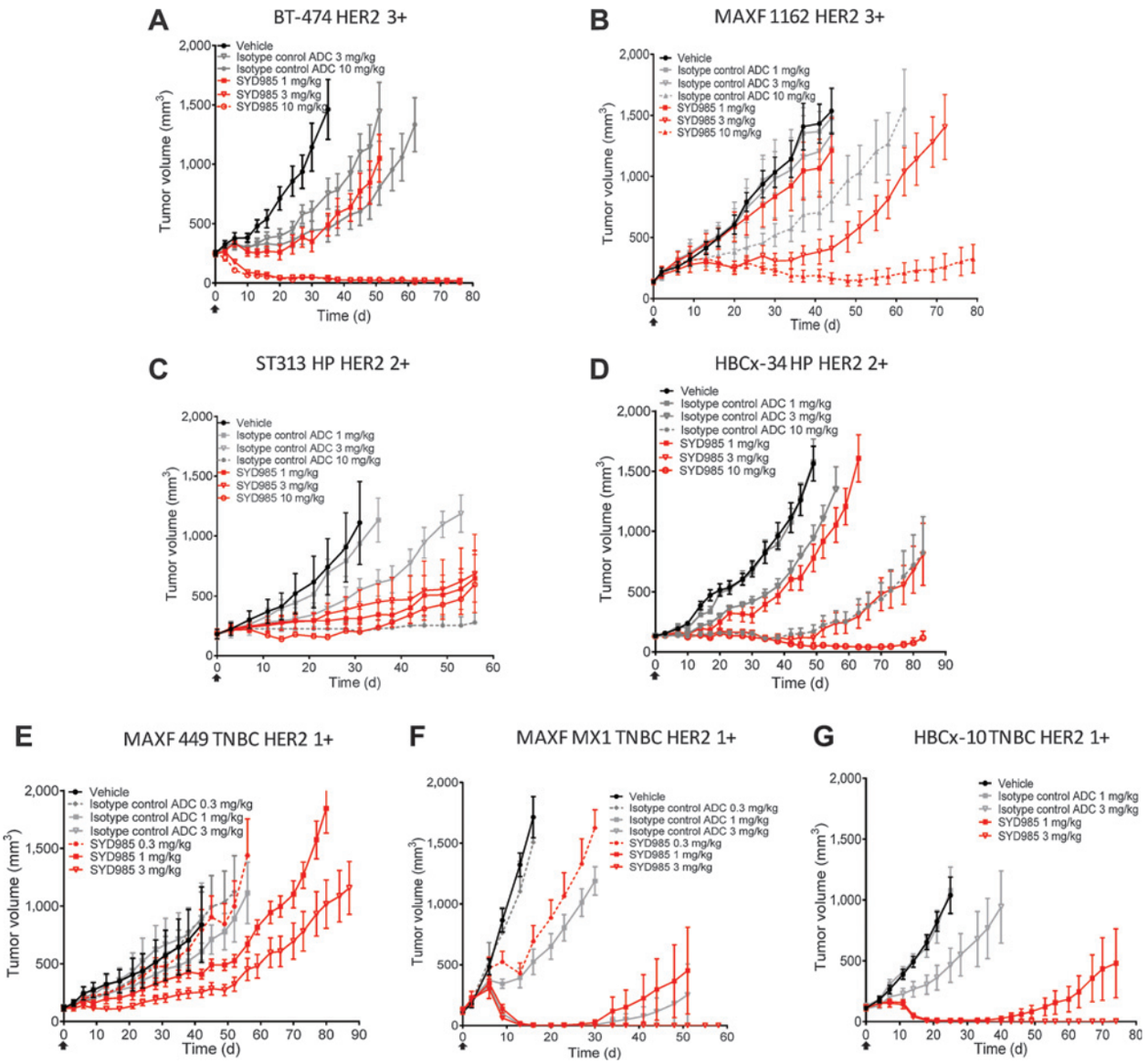

Figure 5.
Antitumor activity of SYD985 compared with isotype control ADC in BT-474 xenograft tumor model (A) and in breast cancer PDX models with different levels of HER2 expressions (B–G). Only isotype control ADC data in the BT-474 model were generated in a separate study (A). All other isotype controls were included within the experiment shown in Fig. 4.

Discussion

To assess the therapeutic value of SYD985 for treatment of patients with breast cancer, we compared its preclinical antitumor activity head-to-head to that of T-DM1 in a series of high and low HER2-expressing breast cancer PDX models. In addition, we have performed mechanistic studies *in vitro* comparing SYD985 to T-DM1 for cytotoxic potency, protease sensitivity, and bystander induction.

SYD985 and T-DM1 share trastuzumab as the targeting mAb, and indeed binding affinities and internalization of the ADCs on several cell lines *in vitro* were similar. Thus, differences between both ADCs should most likely be attributed to either the linker and/or the toxin. Small differences were evident for the respective *in vitro* cytotoxicity in high-expressing HER2 (3+) cell lines, and antitumor activity studies *in vivo* in high HER2-expressing breast cancer xenografts. For both ADCs, these data are in line with previous publications (12, 26–28), although this first head-to-head comparison presented here shows that SYD985, especially *in vivo*, is more active than T-DM1 in high HER2-expressing tumors.

More striking differences were observed in studies in low HER2-expressing cell lines and tumors. SYD985 is a 3- to 50-fold more cytotoxic than T-DM1 in low HER2-expressing (2+/1+) cell lines. Similar binding and internalization profiles of SYD985 and T-DM1 do not explain the difference in cytotoxicity potencies.

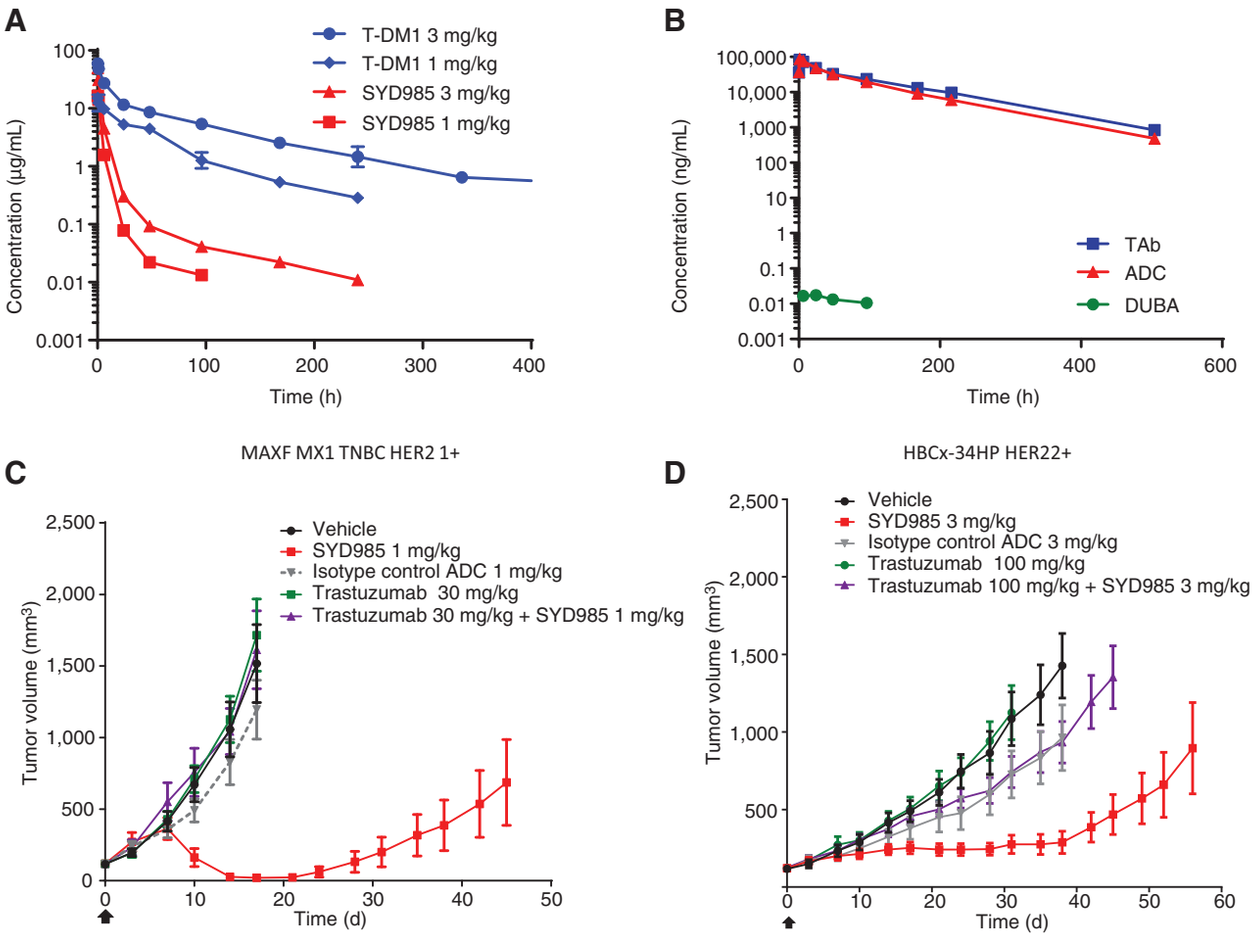

Figure 6.
A, mean ADC (SYD985-conjugated antibody or T-DM1 equivalents) plasma concentrations in BT-474 tumor-bearing mice after a single intravenous bolus injection of SYD985 or T-DM1 at 1 or 3 mg/kg (dose normalized from 5 mg/kg; ±SEM, $n = 3$). B, mean ADC (SYD985-conjugated antibody), TAb, and DUBA plasma concentrations in female cynomolgus monkeys after a single intravenous injection of 3 mg/kg SYD985 (±SEM, $n = 5$). C, antitumor activity of SYD985 at 1 mg/kg (MAXF-MX1) or 3 mg/kg (HBCx-34; D) was blocked by a pretreatment of 30 or 100 mg/kg trastuzumab, respectively.

Also, the payload per Ab cannot explain this difference because T-DM1 carries a mean of 3.7 maytansinoid molecules per ADC molecule versus a mean of 2.8 *seco*-DUBA moieties per molecule SYD985. Apparently, at least for the cell lines tested, cell-permeable duocarmycin *seco*-DUBA as released from SYD985 in endosomes and lysosomes is more efficient in cell killing than the maytansinoid payload which becomes available after complete lysosomal degradation of T-DM1 (29, 30). The nature of toxicity that both toxins induce is indeed different as the payload of T-DM1 is an antimitotic agent preventing microtubule assembly and thereby precluding mitosis in dividing cells (29, 30), whereas the toxic payload of SYD985 is a duocarmycin which alkylates DNA resulting in DNA damage, mitochondrial stress, impaired DNA transcription, and ultimately cell death in both dividing and nondividing cells. Potencies of the respective payloads might be different, but this is hard to assess as the free maytansine payload (carrying the lysine-conjugated linker) is cell impermeable and therefore will show an irrelevantly low *in vitro* cytotoxic activity.

Antitumor effects of SYD985 *in vivo*, also in the low HER2-expressing PDX models, were largely mediated through HER2, as demonstrated by two independent approaches, that is, the use of nonbinding isotype control ADCs and the blocking experiments where a trastuzumab pretreatment blocked SYD985-mediated antitumor activity. Differences in antitumor activities became qualitative when SYD985 and T-DM1 were studied for *in vivo* effects in low HER2-expressing breast cancer PDX models, where SYD985 shows potent antitumor activity and T-DM1 is inactive. *In vitro* data that might contribute to this striking difference *in vivo* includes sensitivity of the linker in SYD985 for cathepsin B cleavage and potent bystander killing observed for SYD985. T-DM1 contains a noncleavable linker which depends on complete digestion of the antibody moiety in lysosomes (31). The resulting DM1-containing lysine derivates induce cytotoxicity, however, they cannot or poorly diffuse across the plasma membrane outside the cell (22) which is in line with lack of bystander killing in our *in vitro* studies. In SYD985, a cleavable dipeptide valine-citrulline linker is used. Linker cleavage by cysteine proteases, such as cathepsin B, present in early- and late endosomes and lysosomes, results in subsequent release of membrane-permeable active toxin. This enables cell killing of HER2-positive cells but also cell death of neighboring

nonantigen-expressing cells, in line with results of bystander studies in this paper.

Proteases, like cathepsin B, also reside in the interstitium of tumors. They are highly expressed in a wide variety of tumors, including breast cancer tumors, and secreted by malignant cells (18, 19, 32). Extracellular cleavage of vc-*seco*-DUBA may therefore induce a bystander effect where not only the HER2-targeted tumor cell is killed, but also neighboring cells. This additional mechanism for bystander killing is a possible explanation for the observed difference in antitumor activity of SYD985 compared with T-DM1 in low HER2-expressing and/or heterogeneous tumors. These data are in line with a previous publication where efficacy of ADCs with cleavable linkers were shown to be less dependent on target expression than ADCs with noncleavable linkers (33). This is also illustrated by the observed antitumor activity of the nonbinding isotype control of SYD985 that indicated that SYD985-mediated antitumor activity was not exclusively target mediated.

As was described previously (12), SYD985 shows a poor stability in mouse plasma and consequently poor kinetics in mice leading to a relatively low exposure. We have shown that the poor PK of SYD985 is due to the presence of a mouse-specific carboxylesterase, CES1c, which is not expressed in human or cynomolgus monkey (12, 34, 35). Currently the exact cleavage site is unconfirmed. Possibly, CES1c hydrolyzes the carbamate bond connecting the alkylating moiety of the duocarmycin to the linker (Fig. 1). CES1c activity and subsequent rapid cleavage of the linker drug in SYD985 lead to early release of active toxin in mouse plasma. In theory, active toxin in plasma in vicinity of the tumor might contribute to antitumor activity of SYD985, as mentioned previously (12). Experiments in the present paper showed that a high dose of trastuzumab blocks antitumor activity of an active dose of SYD985 in two PDX models. This demonstrates that (i) active toxin liberated in plasma or in close vicinity of the tumor does not contribute to antitumor activity and (ii) antitumor activity of SYD985 is largely HER2 mediated.

The exposure in terms of AUC does drive *in vivo* antitumor activity of SYD985 (12) as was also demonstrated for T-DM1 (23, 24). The strong antitumor activity of SYD985 *in vivo* in mice, is striking, especially if one compares the ADC (conjugated antibody) exposures for both ADCs which is, in mice, approximately 10-fold lower for SYD985 compared with T-DM1. Apart from that, CES1c-mediated release of the toxin in mice is accompanied by a substantial increase in naked mAb, which competes for the same HER2-binding sites and is inactive in these PDX models. Thus, efficacy studies with SYD985 *in vivo* in mice most likely lead to an underestimation of antitumor activity in species that will have higher exposure to SYD985, such as human. Monkey PK data and stability studies in human plasma indicate for excellent stability and predictable PK in man (12), thus SYD985 might show an even better efficacy profile in patients. Together, data presented here support the expectation that SYD985 has a clinically relevant efficacy in patients with breast cancer who have cancer tissue with low levels of HER2 expression.

Disclosure of Potential Conflicts of Interest

J.M. Lemmens has ownership interest (including patents) in Synthon. No potential conflicts of interest were disclosed by the other authors.

Authors' Contributions

Conception and design: W.H.A. Dokter, M.M.C. van der Lee, P.G. Groothuis, R. Ubink, D.F. Egging, P.H. Beusker, P. Goedings, G.F.M. Verheijden, J.M. Lemmens

Development of methodology: M.M.C. van der Lee, R. Ubink, D.F. Egging, D. van den Dobbelsteen, P.H. Beusker

Acquisition of data (provided animals, acquired and managed patients, provided facilities, etc.): P.G. Groothuis, D. van den Dobbelsteen

Analysis and interpretation of data (e.g., statistical analysis, biostatistics, computational analysis): W.H.A. Dokter, M.M.C. van der Lee, P.G. Groothuis, R. Ubink, M.A.J. van der Vleuten, T.A. van Achterberg, E.M. Loosveld, D.C.H. Jacobs, M. Rouwette, D.F. Egging, D. van den Dobbelsteen, P.H. Beusker, P. Goedings, G.F.M. Verheijden

Writing, review, and/or revision of the manuscript: W.H.A. Dokter, M.M.C. van der Lee, P.G. Groothuis, R. Ubink, D. Damming, D.F. Egging, D. van den Dobbelsteen, P.H. Beusker, P. Goedings, G.F.M. Verheijden, J.M. Lemmens, M. Timmers

Study supervision: W.H.A. Dokter, M. Timmers

Acknowledgments

The authors thank Prof. T. Hagemann (London, United Kingdom) for providing access to CES1c knockout mice.

Grant Support

This work was financially supported by Synthon Biopharmaceuticals BV.

The costs of publication of this article were defrayed in part by the payment of page charges. This article must therefore be hereby marked *advertisement* in accordance with 18 U.S.C. Section 1734 solely to indicate this fact.

Received October 9, 2014; revised December 22, 2014; accepted December 22, 2014; published OnlineFirst January 14, 2015.

References

1. Chari RVJ, Miller ML, Widdison WC. Antibody-drug conjugates: an emerging concept in cancer therapy. Angew Chem Int Ed 2014;53:3796–827
2. Gopal AK, Ramchandren R, O'Conner OA, Berryman RB, Advani RH, Chen R, et al. Safety and efficacy of brentuximab vedotin for Hodgkin lymphoma recurring after allogeneic stem cell transplantation. Blood 2012;120:560–8.
3. Younes A, Gopal AK, Smith SE, Ansell SM, Rosenblatt JD, Savage KJ, et al. Results of a pivotal Phase II study of brentuximab vedotin for patients with relapsed or refractory Hodgkin's lymphoma. J Clin Oncol 2012;30:2183–9.
4. Pro B, Advani R, Brice P, Bartlett NL, Rosenblatt JD, Illidge T, et al. Brentixumab-vedotin (SGN-35) in patients with relapsed or refractory systemic anaplastic large-cell lymphoma: results of a phase II study. J Clin Oncol 2012;30:2190–6.
5. Burris HA III, Rugo HS, Vukelja SJ, Vogel CL, Borson RA, Limentani S, et al. Phase II study of the antibody drug conjugate trastuzumab-DM1 for the treatment of human epidermal growth factor receptor 2 (HER2) – positive breast cancer after prior HER2-directed therapy. J Clin Oncol 2011;29:398–405.
6. Krop IE, LoRusso P, Miller KD, Modi S, Yardley D, Rodriguez G, et al. A Phase II study of trastuzumab emtansine in patients with human epidermal growth factor receptor 2 – positive metastatic breast cancer who were previously treated with trastuzumab, lapatinib, an anthracycline, a taxane, and capecitabine. J Clin Oncol 2012;30:1–9.
7. Verma S, Miles D, Gianni L, Krop IE, Welslau M, Baselga J, et al. Trastuzumab Emtansine for HER2-positive advanced breast cancer. N Engl J Med 2012;367:1783–91.
8. Hurvitz SA, Dirix L, Kocsis J, Bianchi GV, Lu J, Vinholes J, et al. Phase II randomized study of trastuzumab emtansine versus trastuzumab

vplus docetaxel in patients with human epidermal growth factor receptor 2-positive metastatic breast cancer. J Clin Oncol 2013;31: 1157–63.
9. Slamon DJ, Godolphin W, Jones LA, Holt JA, Wong SG, Keith DE, et al. Studies of the HER2/neu proto-oncogene in human breast and ovarian cancer. Science 1989;244:707–12.
10. Owens MA, Horten BC, Da Silva MM. HER2 amplification ratios by fluorescence in situ hybridization and correlation with immunohistochemistry in a cohort of 6556 breast cancer tissues. Clin Breast Cancer 2004;5:63–9.
11. Press MF, Sauter G, Bernstein L, Villalobos IE, Mirlacher M, Zhou JY, et al. Diagnostic evaluation of HER-2 as a molecular target: an assessment of accuracy and reproducibility of laboratory testing in large, prospective, randomized clinical trials. Clin Cancer Res 2005;11:6598–607.
12. Dokter W, Ubink R, van der Lee M, van der Vleuten M, van Achterberg T, Jacobs D, et al. Preclinical profile of SYD983/SYD985, a new generation HER2 targeting antibody-drug conjugate. Mol Cancer Ther 2014;13:2618–29.
13. Beusker PH, Coumans RGE, Elgersma RC, Menge WMPB, Joosten JAF, Spijker HJ, et al. Novel CC-1065 analogs and their conjugates. Int Patent Publ WO2010/062171. 2010 Jun 3.
14. Beusker PH, Coumans RGE, Elgersma RC, Menge WMPB, Joosten JAF, Spijker HJ, et al. Novel conjugates of CC-1065 analogs and bifunctional linkers. Int Patent Publ WO2011/133039. 2001 Oct 27.
15. De Groot FMH, Beusker PH, Scheeren JW, de Vos D, van Berkom LWA, Busscher GF, et al. Elongated and multiple spacers in activatible prodrugs. Int Patent Publ WO02/083180. 2002 Oct 24.
16. O'Brien NA, Browne BC, Chow L, Wang Y, Ginther C, Arboleda J, et al. Activated phosphoinositide 3-kinase/AKT signaling confers resistance to trastuzumab but not lapatinib. Mol Cancer Ther 2010;9:1489–502.
17. Barok M, Tanner M, Koninki K, Isola J. Trastuzumab-DM1 causes tumour growth inhibition by mitotic catastrophe in trastuzumab-resistant breast cancer cells *in vivo*. Breast Cancer Res 2011;13:R46.
18. Rohzin J, Sameni M, Ziegler G, Sloane BF. Pericellular pH affects distribution and secretion of cathepsin B in malignant cells. Cancer Res 1994;54:6517–25.
19. Aggarwal N, Sloane BF. Cathepsin B: multiple roles in cancer. Proteomics Clin Appl 2014;8:427–37.
20. Doronina SO, Toki BE, Torgov MY, Mendelsohn BA, Cerveny CG, Chace DF, et al. Development of potent monoclonal antibody auristatin conjugates for cancer therapy. Nat Biotech 2003;21:778–84.
21. Kellogg BA, Garrett L, Kovtun Y, Lai KC, Leece B, Miller M, et al. Disulfide-linked antibody-maytansinoid conjugates: optimization of *in vivo* activity by varying the steric hindrance at carbon atoms adjacent to the disulfide linkage. Bioconjug Chem 2011;22:717–27.
22. Kovtun YV, Audette CA, Ye Y, Xie H, Ruberti MF, Phinney SJ, et al. Antibody-drug conjugates designed to eradicate tumors with homogeneous and hetergeneous expression of the target antigen. Cancer Res 2006;66:3214–21.
23. Jumbe NL, Xin Y, Leipold DD, Crocker L, Dugger D, Mai E, et al. Modeling the efficacy of trastuzumab-DM1, an antibody drug conjugate, in mice. J Pharmacokinet Pharmacodyn 2010;37:221–42.
24. Ersboll J, Melchiorri D, editors. Assessment report Kadcyla [Internet]. London: European Medicines Agency; 2013 [cited 2013 Sept 19]. Available from: http://www.ema.europa.eu/docs/en_GB/document_library/EPAR_-_Public_assessment_report/human/002389/WC500158595.pdf.
25. Poon KA, Flagella K, Beyer J, Tibbits J, Kaur S, Saad O, et al. Preclinical safety profile of trastuzumab-emtansine (T-DM1): mechanism of action of its cytotoxic component retained with improved tolerability. Toxicol Appl Pharmacol 2013;273:298–313.
26. Junttila TT, Li G, Parsons K, Phillips GL, Sliwkowski MX. Trastuzumab-DM1 (T-DM1) retains all the mechanism of action of trastuzumab and efficiently inhibits growth of lapatinib insensitive breast cancer. Breast Cancer Res Treat 2011;128:347–56.
27. Lewis Phillips GD, Li G, Dugger DL, Crocker LM, Parsons KL, Mai E, et al. Targeting HER2-positive breast cancer with trastuzumab-DM1, an antibody-cytotoxic drug conjugate. Cancer Res 2008;68: 9280–90.
28. Lewis Phillips GD, Fields CT, Li G, Dowbenko D, Schaefer G, Miller K, et al. Dual targeting of HER2-positive cancer with trastuzumab-emtansine and pertuzumab: critical role for neuregulin blockade in antitumor response to combination therapy. Clin Cancer Res 2013;20:1–13.
29. Chari RVJ, Martell BA, Gross JL, Cook SB, Shah SA, Blattler WA, et al. Immunoconjugates containing novel maytansinoids: promising anticancer drugs. Cancer Res 1992;52:127–31.
30. Remillard S, Rebhun LI, Howie GA, Kupchan SM. Anti-mitotic activity of the potent tumor inhibitor maytansine. Science 1975;189:1002–5.
31. Burris HA III, Tibbitts J, Holden SN, Sliwkowski MX, Lewis Phillips GD. Trastuzumab Emtansine (T-DM1): a novel agent for targeting HER2+ breast cancer. Clin Breast Cancer 2011;11:275–82.
32. Rothberg JM, Bailey KM, Wojtkowiak W, Ben-Nun Y, Bogyo M, Weber E, et al. Acid-mediated tumor proteolysis: contribution of cysteine cathepsins. Neoplasia 2013;15:1125–37.
33. Polson AG, Calemine-Fenaux J, Chan P, Chang W, Christensen E, Clark S, et al. Antibody-drug conjugates for the treatment of non-Hodgkin's lymphoma: target and linker-drug selection. Cancer Res 2009;69:2358–64.
34. Li B, Sedlacek M, Manoharan I, Boopathy R, Duysen EG, Masson P, et al. Butyrylcholinesterase, paraoxonase, and albumin esterase, but not carboxylesterase, are present in human plasma. Biochem Pharmacol 2005;70: 1673–84.
35. Duysen EG, Koentgen F, Williams GR, Timperley CM, Schopfer LM, Cerasoli DM, et al. Production of ES1 plasma carboxylesterase knockout mice for toxicity studies. Chem Res Toxicol 2011;24:1891–8.